Analytica Chimica Acta 1328 (2024) 343159

Contents lists available at ScienceDirect

Analytica Chimica Acta

journal homepage: www.elsevier.com/locate/aca

Multivariate curve resolution-alternating least-squares and second-order advantage in first-order calibration. A systematic characterisation for three-component analytical systems

Fabricio A. Chiappini [a,b], Licarion Pinto [c], Mirta R. Alcaraz [a,b], Nematollah Omidikia [d], Hector C. Goicoechea [a,b,e], Alejandro C. Olivieri [b,f,*]

[a] Laboratorio de Desarrollo Analítico y Quimiometría (LADAQ), Cátedra de Química Analítica I, Facultad de Bioquímica y Ciencias Biológicas, Universidad Nacional del Litoral, Ciudad Universitaria, Santa Fe, S3000ZAA), Argentina
[b] Consejo Nacional de Investigaciones Científicas y Técnicas (CONICET), Godoy Cruz 2290, CABA, (C1425FQB), Argentina
[c] Laboratório de tecnologia analítica de processos, Departamento de química analítica, Instituto de Química, Universidade do Estado do Rio de Janeiro (UERJ), Rio de Janeiro, Brazil
[d] Department of Marine Microbiology & Biogeochemistry, NIOZ Royal Netherlands Institute for Sea Research, 't Horntje (Texel), the Netherlands
[e] Departamento de Química Analítica, Universidad de Extremadura, Badajoz, 06006, Spain
[f] Departamento de Química Analítica, Facultad de Ciencias Bioquímicas y Farmacéuticas, Universidad Nacional de Rosario, Instituto de Química de Rosario (IQUIR-CONICET), Suipacha 531, Rosario, (S2002LRK), Argentina

HIGHLIGHTS

- First-order datasets with different selectivity patterns are investigated.
- Multivariate curve resolution may achieve the second-order advantage for these data.
- Rotational ambiguity effects are studied in three-component systems.
- Areas of feasible solutions are analyzed.

GRAPHICAL ABSTRACT

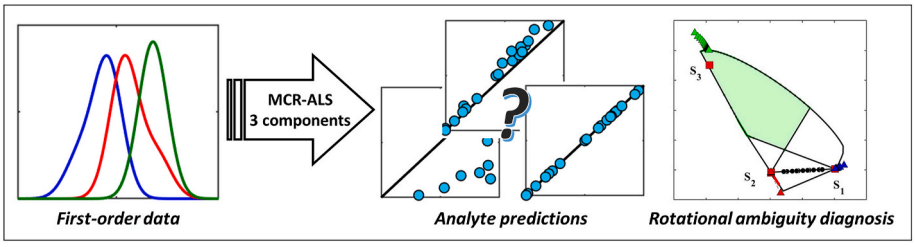

ARTICLE INFO

Handling Editor: Prof. L. Buydens

Keywords:
Calibration
Unfolded multivariate curve resolution-alternating least-squares
Rotational ambiguity
Analyte selectivity
Local rank

ABSTRACT

Background: Recent interest has been focused on the application of multivariate curve resolution-alternating least-squares (MCR-ALS) to systems involving the measurement of first-order and non-bilinear second-order data. The latter pose important challenges to bilinear decomposition models, due to the phenomenon of rotational ambiguity in the solutions, even under the application of the full set of chemical constraints that is usually employed in MCR-ALS calibration.
Results: After the analysis of several simulated and experimental datasets, important conclusions regarding the role of the selectivity patterns in the constituent spectra have been drawn concerning the achievement of the second-order advantage. Theoretical considerations based on the calculation of the areas of feasible solutions helped to support the observations regarding the predictive ability of MCR- ALS in the various datasets.

* Corresponding author. Consejo Nacional de Investigaciones Científicas y Técnicas (CONICET), Godoy Cruz 2290, CABA, (C1425FQB), Argentina.
E-mail address: olivieri@iquir-conicet.gov.ar (A.C. Olivieri).

https://doi.org/10.1016/j.aca.2024.343159
Received 7 March 2024; Received in revised form 20 August 2024; Accepted 25 August 2024
Available online 26 August 2024

Significance: The understanding of the impact of rotational ambiguity in obtaining the second-order advantage with both first-order and non-bilinear second-order data is of paramount importance in the future development of analytical protocols of complex samples.

1. Introduction

In recent decades, multivariate curve resolution-alternating least-squares (MCR-ALS) has gained tremendous relevance in the analytical chemistry community. Due to significant advances in the chemometric field, MCR-ALS has been thoroughly characterised, and theoretical and methodological contributions have been continuously reported [1]. For these reasons, the application of this strategy to model second-order instrumental data has triggered the development of numerous calibration methodologies, due to the ability of MCR-ALS to exploit the well-known analytical second-order advantage, i.e., the possibility of quantifying an analyte of interest, even in the presence of unexpected or uncalibrated components [2]. Moreover, as extensively reviewed, the extended MCR-ALS formulation constitutes a more flexible modelling approach than classical trilinear calibration models, since it allows to deal with the lack of signal synchronisation in one of the experimental modes [3].

Mathematically, MCR-ALS consists of a bilinear decomposition of a two-way data array. One of the main disadvantages is that it may suffer from the rotational ambiguity phenomenon (RA) due the lack of uniqueness in the solutions [4–10]. When this occurs, the analytical performance of an MCR-ALS-based methodology can be severely affected [11]. The extent of the RA can be mitigated when constraints are imposed during the ALS optimisation, e.g., non-negativity, unimodality, selectivity, local rank, correspondence between species and samples, mass-balance, trilinearity, area correlation, among others [12, 13]. However, it is interesting to point out that, under certain circumstances, the use of constraints does not remove the RA completely.

It has been experimentally shown that in systems with rank deficiency, e.g., data with complete overlap of constituent profiles in one of the data modes, the MCR-ALS solutions display a large degree of RA [14]. Nevertheless, it is possible to generate MCR-ALS-based calibration models with satisfactory analytical performance, even in the presence of a substantial RA. In these scenarios, constraints and initialisation procedures play a critical role [15].

The diagnosis of RA can be carried out both analytically and numerically. While simple self-modelling curve resolution (SMCR) methods delimit feasible regions analytically, i.e. Lawton-Sylvester and Borgen-Rajkó plots for two and three-component analytical systems [4, 16], the grid search [9] and the polygon inflation [17] methods use numerical methods to calculate the feasible solutions. The underlying geometrical and algebraic complexity of most of these methods makes diagnosing the extent of RA in multicomponent systems challenging and computationally demanding. Consequently, most algorithms have not been generalised for systems with more than three components. Alternative strategies for multi-component systems have been proposed, such as the MCR-BANDS, N-BANDS and SW-N-BANDS. However, these methods do not retrieve all the feasible solutions, but only the maximum and minimum ones [18–20]. As can be noted, RA is still a matter of debate in the chemometric community.

The particular advantages and flexibility of MCR-ALS have motivated its application to other types of data, such as first-order and unfolded non-bilinear second-order data sets [21,22]. Regarding first-order calibration, it is well-known that classical algorithms, e.g., partial least-squares regression (PLS), are severely limited in their capacity to accurately predict an analyte in the presence of uncalibrated substances. On the other hand, the application of conventional second-order chemometric models to non-bilinear second-order data is extremely limited, because most methods rely on the hypothesis of low-rank bi- or trilinearity. Nevertheless, to the best of our knowledge, no general method has been reported to properly model and exploit the second-order advantage in non-bilinear scenarios. Recently, our group has thoroughly investigated under which circumstances MCR-ALS can adequately predict the concentration of an analyte in the presence of non-calibrated constituents in the case of two-component systems, having a single analyte and a single interferent [23,24]. In the latter work, it was demonstrated that, although a substantial extent of RA persists in first-order (or unfolded second-order) calibration datasets, MCR-ALS can satisfactorily achieve predictions under the following conditions: (i) the analyte exhibits a selective signal region and (ii) when initial estimates are calculated through the purest variables method, the initialisation should be conducted with concentration profiles at the purest spectral variables. The second condition exploits the benefit stemming from the first condition, i.e., a selective spectral region, resulting in a concentration profile close to that for the pure analyte. Previous findings also showed that the capacity of MCR-ALS to properly solve these systems is not significantly affected by the level of instrumental noise [23,24].

The present study aims to extend the previous results to three-component analytical systems, involving two analytes and one interferent. Different simulated datasets were generated and analyzed with a special focus on signal selectivity patterns. The diagnosis of RA was accomplished through Borgen-Rajkó plots, which were drawn to investigate the feasible regions in each calibration scenario and to interprete the predictive performance of MCR-ALS. The outcomes were then validated through the study of two experimental systems. It is important to remark that this work is devoted to first-order data, but the results can be naturally extended to unfolded non-bilinear second-order data.

2. Theory

2.1. Nomenclature and general considerations

In first-order calibration, vectorial signals measured at J instrumental sensors are generated for a group of I samples, which can be disposed in a single matrix $\mathbf{D}$ of size $I \times J$. This matrix can then be submitted to MCR-ALS decomposition through [12]:

$$\mathbf{D} = \mathbf{C}\,\mathbf{S}^{\mathrm{T}} + \mathbf{E} \tag{1}$$

where $\mathbf{C}$ and $\mathbf{S}$ of size $I \times A$ and $J \times A$, respectively, capture the contribution and the pure profiles of A responsive components, and $\mathbf{E}$ ($I \times J$) captures the model error.

In this calibration approach, two types of vectorial signals are considered: $\mathbf{x}_{cal}$, corresponding to calibration samples with the pure analytes and $\mathbf{x}_{test}$ corresponding to the test samples, in which uncalibrated substances may occur. Thus, the experimental matrix $\mathbf{D}$ in Eq. (1), generated for N calibration samples and one generic test sample, can be described in MATLAB notation as $\mathbf{D} = [\mathbf{x}_{test}; \mathbf{x}_{cal,1}; \mathbf{x}_{cal,2}; \ldots; \mathbf{x}_{cal,N}]$.

The matrices $\mathbf{C}$ and $\mathbf{S}^{\mathrm{T}}$ from Eq. (1) are calculated using the ALS optimisation procedure. After convergence, the columns of $\mathbf{C}$ contain the so-called sample scores, which are used for further prediction: a pseudo-univariate calibration line is built with the calibration scores, whereas the test score is used to estimate the analyte concentration.

Under the above notation, in a first-order scenario, the matrix $\mathbf{D}$ comprises the instrumental and concentration information in the row and column direction, respectively. By analogy to second-order calibration with the extended MCR-ALS model form, columns and rows represent the augmented and the non-augmented modes, respectively. However, throughout this work, they are referred to as concentration (or

sample) **C** and instrumental **S** directions to avoid name conflicts.

The same modelling approach represented by Eq. (1) can be applied to non-bilinear second-order data. If a set of $J \times K$ response matrices are measured for I samples and unfolded into vectors, then a matrix **D** of size $I \times JK$ can be generated. At this point, it is important to highlight that the proof of concept carried out for both first-order and non-bilinear second-order data in previous works for two-component calibration systems have yielded perfectly equivalent results [23,24]. From this point of view, it can be stated that when non-bilinear second-order data are unfolded, they can be treated as first-order data. However, it is logical to expect that unfolded second-order data would present additional advantages over genuine first-order data, considering the improvement in selectivity and other analytical figures of merit (AFOMs) and the variety of strategies that the MCR-ALS method presents in the context of second-order calibration. These aspects have not been fully explored yet and are not the objective of the current report.

On the other hand, it is also important to mention that the ability of MCR-ALS to successfully predict an analyte in the presence of non-calibrated components using first-order data can be considered as an extension of the second-order advantage. This expression is appropriate for the case of non-bilinear second-order data. However, when genuine first-order data are involved, referring to it as interference-free calibration would be more appropriate to avoid a conceptual inconsistency.

Based on MCR-ALS decomposition, the specific modelling approach recently discussed in the literature both for first-order and unfolded non-bilinear second-order share the following two main characteristics: (i) there is a single instrumental mode; (ii) analytical information about potential interferents is not included in the calibration samples. In particular, in previous studies, the application of MCR-ALS to unfolded non-bilinear second-order data has been named as unfolded- or U-MCR-ALS, by analogy to the well-known U-PLS-RBL chemometric method.

2.2. Selectivity and local rank

In previous works, the selectivity was considered a key factor in evaluating the ability of MCR-ALS to properly decompose first-order calibration datasets. In multivariate calibration, selectivity is a parameter that measures the ratio of net to pure analyte signal, and it varies between 0 (no selectivity) and 1 (full selectivity). Mathematically, the selectivity (*sel*) of the *i*-th analyte in a mixture can be estimated as:

$$sel = \frac{\mathbf{1}}{\left\| \mathbf{s}_i * \sqrt{\left(\mathbf{S}_0^{\mathrm{T}}\mathbf{S}_0\right)^{-1}_{ii}} \right\|} \tag{2}$$

where $\mathbf{s}_i$ is a vector containing the normalised pure profile of the analyte, $\mathbf{S}_0$ is a matrix containing the normalised pure profiles of all the constituents in the mixture; the subindex *ii* indicates the *i*-th diagonal element of the inverse of a square matrix $\left(\mathbf{S}_0^{\mathrm{T}}\mathbf{S}_0\right)$ and $\|\|$ indicates the Euclidean norm. From the experimental point of view, both the shape and the degree of overlap between the signal profiles of the responsive constituents contribute to the selectivity of each component. Therefore, having a non-zero selectivity for a given analyte is a necessary condition to ensure a proper resolution when signals are submitted to a chemometric decomposition. Moreover, if more instrumental modes are available, it is likely that the selectivity of a component of interest will increase [25].

In the context of MCR-ALS calibration, two concepts related to the idea of selectivity appear, which can be incorporated as model constraints to minimise the extent of RA. In calibration datasets with a mixture of components, the selectivity and local rank constraints refer to data regions where one or more components are absent, i.e., regions where the rank is lower than the total rank of the dataset. According to the nomenclature proposed by Tauler and de Juan [12], when a single component is present in a certain region, there is a selective window for that component. Besides, in regions where some components are absent, there is a window of local rank. For example, the concentration mode is selective for a given analyte when it is present in pure form in one or more samples. This idea of selectivity is also named sample selectivity and, in MCR modelling, it can be incorporated into the ALS procedure as the constraint of correspondence between species and samples.

On the other hand, the signal selectivity constraint can be applied when there are one or more sensor windows for a given instrumental mode where the contribution to the total instrumental signal is only due to a single constituent. This idea of selectivity comes into play to judge the resolution capacity of MCR-ALS. However, with the aim of avoiding name conflicts and confusion with the selectivity defined according to Eq. (2), the sensor windows in the instrumental mode where all components are absent except for one will be here referred as regions of local rank 1. It is evident that when there is a region of local rank 1 for a given analyte, the selectivity defined according to Eq. (2) is larger than zero. The reciprocal is not necessarily true.

It should be remarked that in this work, the term 'rank' will be used to characterise the rank of the dataset formed by all the calibration samples together with the test sample to be predicted, i.e., the **D** matrix, and not to refer to the rank of a vectorial signal of a single sample. Furthermore, it should be emphasised that selectivity/local rank information will not be incorporated during MCR-ALS in this research. However, the pure variable selection directly enjoys from such a local rank 1 region and affects the calibration outputs.

As stated before, previous works have theoretically and experimentally demonstrated that, under proper initialisation and constraints, even in the presence of non-unique solutions, MCR-ALS is capable of yielding satisfactory analytical predictions in a two-component system when the analyte of interest exhibits a region of local rank 1 [23,24]. This is the hypothesis that is under study in the current investigation for three-component analytical systems.

2.3. Borgen-Rajkó plots and RA diagnosis

RA is related to the existence of a range of possible solutions for the bilinear decomposition of Eq. (1). It has been previously demonstrated that in the context of MCR-ALS, a unique bilinear decomposition of the matrix **D** is never achieved for cases with rank overlap condition [15]. However, under certain circumstances, satisfactory analytical predictions are still possible. Therefore, as is usual in MCR modelling, it is of paramount importance to characterise the area of feasible solutions (AFS), as a way of evaluating the RA extent.

Borgen-Rajkó plots refer to a geometrical construction of the AFS resulting from a non-negative factorisation of a spectral data matrix for a three-component system. This strategy is based on the theory developed by Lawton and Sylvestre in 1971 for two components, generalised later by Borgen and Rajkó [26]. Specifically, the building of three-component plots of AFS involve the calculation of the projections of the feasible profiles onto the space spanned by the principal components of the data matrix. This produces a set of three values per feasible profile, which upon suitable scaling render two coordinates per profile. Borgen-Rajkó plots graphically represent the AFS points using those two coordinates in a two-dimensional map. Mathematical details are beyond the scope of this work and the readers may refer to the original publications. These plots depict the microstructure of three-component cases illustrating feasible regions and inner and outer polygons achieved through a computational geometry calculation. The inner polygon is the convex set of row or column spaces of the recorded dataset delineated by the convex hull [16] featuring pure profiles on its vertices [26]. On the other hand, the outer polygon is the non-negativity boundary. Notably, the Borgen-Rajkó plot can be generated for both the row and column space of the dataset, and a robust relationship known as duality connects these two spaces [27]. This duality allows for thoroughly examining the initialisation effects and convergence properties of bilinear methods.

3. Experimental section

In this work, simulated and real datasets were used to illustrate a variety of first-order calibration scenarios with three components. A systematic study was conducted to investigate the ability of MCR-ALS to deal with two-analyte calibrations in the presence of an unexpected component. It is evident that the conclusions that can be drawn from the analysis of cases for one of the analytes are extended equivalently for the other analyte. For this reason, all the considered cases refer only to the prediction of one of the analytes in each chemical system, referred to as analyte 1.

3.1. Simulated data

Simulated first-order spectral datasets with three components were produced, by generating proper matrices **C** and **S**, as appropriate [see Eq. (1)]. Two calibration schemes were considered, S1 and S2, which we call simultaneous and individual calibration schemes, respectively. In S1, calibration samples contain both analytes, each of them in the concentration range of 0–1 arbitrary units, corresponding to binary mixtures taken from a 5^2 full factorial design with 3 replicates (75 calibration samples in total) The design matrix is provided in the Supplementary Material. In S2, in contrast, the analytes were individually calibrated. Therefore, two independent calibration datasets containing five equidistant levels in triplicates spanning the range 0–1 concentration units were obtained (15 calibration samples). The test sets were common for both calibration schemes: 20 test samples were generated containing both analytes and one interferent as a third component, with concentrations taken randomly and uniformly distributed from the ranges 0–1 units for the analytes and 0.5–1.5 units for the interferent. Notice that when the S2 scheme is considered, only one of the analytes is present in the calibration samples, but the three constituents are in the test samples. For instance, if analyte 1 is to be predicted, analyte 2 is not present in the calibration samples, i.e., it acts as an interferent. However, it is named as analyte 2 to simplify the notation.

For the generation of each dataset, three synthetic pure spectral profiles were designed to give an **S** matrix (50 sensors-length), considering different cases of local rank, i.e., each component exhibiting different windows of individual contribution. If the analyte 1 is to be predicted, four cases can be established. They are illustrated in Fig. 1, where normalised pure profiles for the analyte 1 (blue), the analyte 2 (red), and the interferent (green) are shown: (i) case A, all components are completely overlapped (there is no region of local rank 1 for any of the components); (ii) case B, only the analyte 1 has a spectral region of local rank 1 (ca. from sensor 1 to 17); (iii) case C, both analytes exhibit a region of local rank 1 (ca. from sensor 1 to 17 for the analyte 1 and 44 to 50 for the analyte 2); (iv) case D, same as C, but the interferent has also a spectral selective region (regions of local rank 1 are in the sensor ranges of ca. 1–17, 27–30 and 43–50 for the analyte 1, the analyte 2 and the interferent, respectively).

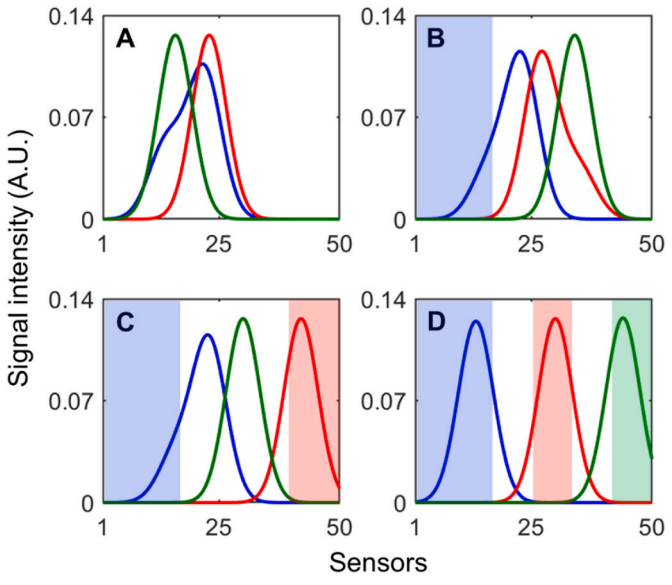

Fig. 1. Unit-concentration spectra of analyte 1 (blue), analyte 2 (red) and interferent (green) used to generate all the simulated systems, considering four cases of local rank: A) case A, none of the components present a region of local rank 1 (all profiles are completely overlapped); B) case B, only analyte 1 has a region of local rank 1; C) case C, both analytes exhibit a region with local rank 1 (regions of pure contribution); D) case D, same as C, but the interferent has also a window of local rank 1. (For interpretation of the references to colour in this figure legend, the reader is referred to the Web version of this article.)

Additionally, to generate **C** matrices, 1×3 vectors comprising the concentration of the three constituents in the test samples were iteratively appended to a calibration matrix of size $n \times 3$, containing n calibration samples, where the first and the second columns included the concentration of each analyte, respectively (according to a given calibration scheme). The third column corresponded to the interferent and, therefore, from row 2 to $n + 1$ it was filled with zeros.

Both in S1 and S2 systems, **C** and **S** matrices were multiplied according to Eq. (1) to give **D** with different properties. This procedure was completed by adding a certain amount of independent and identically distributed (iid) noise, defining a percentage of the mean calibration signal value as noise level as follows: 2, 5 and 10 % were independently evaluated.

As usual in MCR-ALS modelling, calibration-prediction cycles were carried out by processing one test sample at a time. For this reason, a **D** matrix was obtained by multiplying the spectral profiles **S** for a given case of local rank, in each of the conisdered calibration schemes, concentration levels in test samples and levels of noise, with the corresponding **C** matrix, built with the test sample to be predicted (first row) and the calibration samples, as described above. This methodology implied that a total of 24 different simulated systems were submitted to MCR-ALS modelling.

The initial estimates were calculated with concentration profiles at the purest spectral variables, setting the number of MCR components to 3 for S1 and 2 for S2. Further details regarding the number of components and initialisation are given in the next sections. The ALS procedure was conducted under non-negativity constraints in both modes (instrumental signal and concentration) and correspondence between species and samples (sample selectivity). In each calibration-prediction cycle, after convergence, the pseudo univariate calibration line was built with the elements of the estimated matrix **C**, corresponding to the analyte 1 and the test sample score was interpolated to give the analyte prediction. The prediction results for all test samples were used to calculate the percentage relative error of prediction (REP%), according to:

$$\mathrm{REP\%} = \frac{100}{\bar{y}_{cal}} \sqrt{\frac{\sum_{i=1}^{20} (\hat{y}_i - y_i)^2}{20}} \tag{3}$$

where $\hat{y}_i$ and y_i are the predicted and the true concentration of analyte 1 for the i-th test sample, respectively, and $\bar{y}_{cal}$ is the mean concentration of analyte 1 in the calibration set. This parameter served as a statistical indicator to judge the prediction capacity of all MCR-ALS calibration models. The ability of MCR-ALS to solve each artificial system was systematically assessed concerning the local rank patterns and the level of instrumental noise. These results were qualitatively interpreted and explained by estimating the AFS by means of Borgen-Rajkó plots.

3.2. Experimental data

The experimental system E1 consisted of UV spectra obtained for the simultaneous quantification of paracetamol (PAR), caffeine (CAF) and

diclofenac (DCF) in pharmaceutical raw materials and commercial products, reported in Ref. [28]. This system was evaluated as analogous to one of the cases of the S2 calibration scheme. In the present work, DCF and CAF were designated analytes 1 and 2, respectively, while PAR was considered the non-calibrated component. Only the case of DCF prediction is analyzed here. DCF was calibrated in 5 triplicate levels between 1 and 7 ppm, and in the 15 test samples, DCF concentration varied from 1.21 to 3.79 ppm. Table 1 (top) shows the composition of the test samples. The reader is referred to the original publication for more information about experimental conditions.

The second experimental system, E2, consisted of a set of chromatograms obtained at 450 nm emission wavelength (275 nm excitation wavelength) for the quantification of ciprofloxacin (CPF) and ofloxacin (OFL) in the presence of danofloxacin (DNF) as a non-calibrated compound. With this system, both calibration schemes were evaluated. Firstly, in a manner analogous to S1, calibration samples containing CPF and OFL were generated, with concentrations taken from a 3^2 factorial design ranging from 8 to 42 ppm. On the other hand, in analogy with S2, CPF and OFL calibration samples were individually prepared in the concentration range of 10–50 ppm. Additionally, 6 test samples containing CPF, OFL, and DNF mixtures were prepared in the concentrations shown in Table 1 (bottom). Further details about these experiments and the chromatographic conditions can be found in the Supplementary Material. Due to possible misalignments in the chromatographic signals among samples, the chromatograms were submitted to correlation-shifting method [29] to guarantee an adequate data matrix structure. Test chromatograms were individually aligned with the rest of the calibration signals by appropriately trimming extreme data points.

The results of test sample predictions were used to evaluate the prediction capacity in each case. In particular, a REP% value was computed for the case of E1, whereas the average percentage recovery (R%) was calculated with the results of E2 modelling due to the low number of test samples.

$$R\% = \frac{\sum_{i=1}^{I} \frac{\hat{y}_i}{y_i} 100}{I} \quad (4)$$

Table 1
Concentration values in ppm of DCF, CAF and PAR in E1 and OFL, CPF and DNF in E2 used in test samples.

Experimental system 1 (E1)			
Sample	DCF	CAF	PAR
1	1.50	1.50	1.50
2	3.50	1.50	1.50
3	1.50	3.50	1.50
4	3.50	3.50	1.50
5	1.50	1.50	3.50
6	3.50	1.50	3.50
7	1.50	3.50	3.50
8	3.50	3.50	3.50
9	1.21	2.50	2.50
10	3.79	2.50	2.50
11	2.50	1.21	2.50
12	2.50	3.79	2.50
13	2.50	2.50	1.21
14	2.50	2.50	3.79
15	2.50	2.50	2.50
Experimental system 2 (E2)			
Sample	OFL	CPF	DNF
1	25	25	5
2	42	8	5
3	25	25	10
4	25	8	20
5	25	25	20
6	8	25	10

where I is the total number of test samples.

3.3. Software

Data management, pre-processing, simulations, and MCR-ALS analysis were performed in MATLAB R2017b software (The MathWorks Inc., Natick, USA). In particular, MCR-ALS for first-order data was carried out using in-house scripts and the graphical user interface MVC2 [30].

4. Results and discussion

4.1. Simulated data – analytical performance

For the S1 calibration scheme, MCR-ALS models were built with 3 components. The ALS procedure was accomplished with component profiles at the purest variables only with concentration profiles at the purest spectral variables, under non-negativity in both modes and correspondence.

For the calibration of analyte 1 in S2, MCR-ALS modelling was implemented following the same methodology described for S1 but using 2 components. This fact implies that analyte 2 and the interferent, both present in test samples, are jointly modelled as a single non-modelled component. This variant does not alter the results of the predictions of analyte 1 and greatly facilitates the computational implementation of MCR-ALS for S2 datasets. As stated in previous works, MCR cannot distinguish among one or several un-modelled components in test samples in first-order calibration because the rank of the data matrix is equal to the number of calibrated compounds +1, i.e., all contributions in test samples are combined into a single mathematical component.

For each of the local rank cases (A to D) and the three considered instrumental noise levels, a REP% value was computed from the predicted concentrations of analyte 1 (blue profiles in Fig. 1). From the analytical standpoint, a satisfactory REP% value is considered when it is of the order of the level of instrumental noise. The results corresponding to the prediction of analyte 1 in all the simulated systems are numerically summarized in Table 2 and graphically presented in Fig. 2A and B for S1 and S2, respectively.

In the first place, it is interesting to mention that in all cases, the selectivity defined according to Eq. (2), is larger than zero for the analyte 1 (0.11, 0.72, 0.94 and 1.00, for cases A to D, respectively). However, as observed in previous works, in the context of MCR-ALS and first-order calibration, this feature is not enough to guarantee satisfactory predictions when non-calibrated constituents occur.

Table 2
REP% of analyte 1 in the simulated datasets after MCR-ALS modelling, according to S1 and S2 calibration strategies.

Noise level	Case	REP%	
		S_1[a]	S_2[b]
2 %	**A**	>100	>100
	B	18.1	1.1
	C	0.4	0.6
	D	1.4	0.8
5 %	**A**	>100	>100
	B	19.5	1.2
	C	0.9	1.9
	D	3.4	2.2
10 %	**A**	>100	>100
	B	21.3	2.0
	C	2.8	4.3
	D	6.4	4.4

[a] Both analytes are present in the calibration samples (simultaneous calibration).
[b] Only analyte 1 is present in the calibration samples (individual calibration).

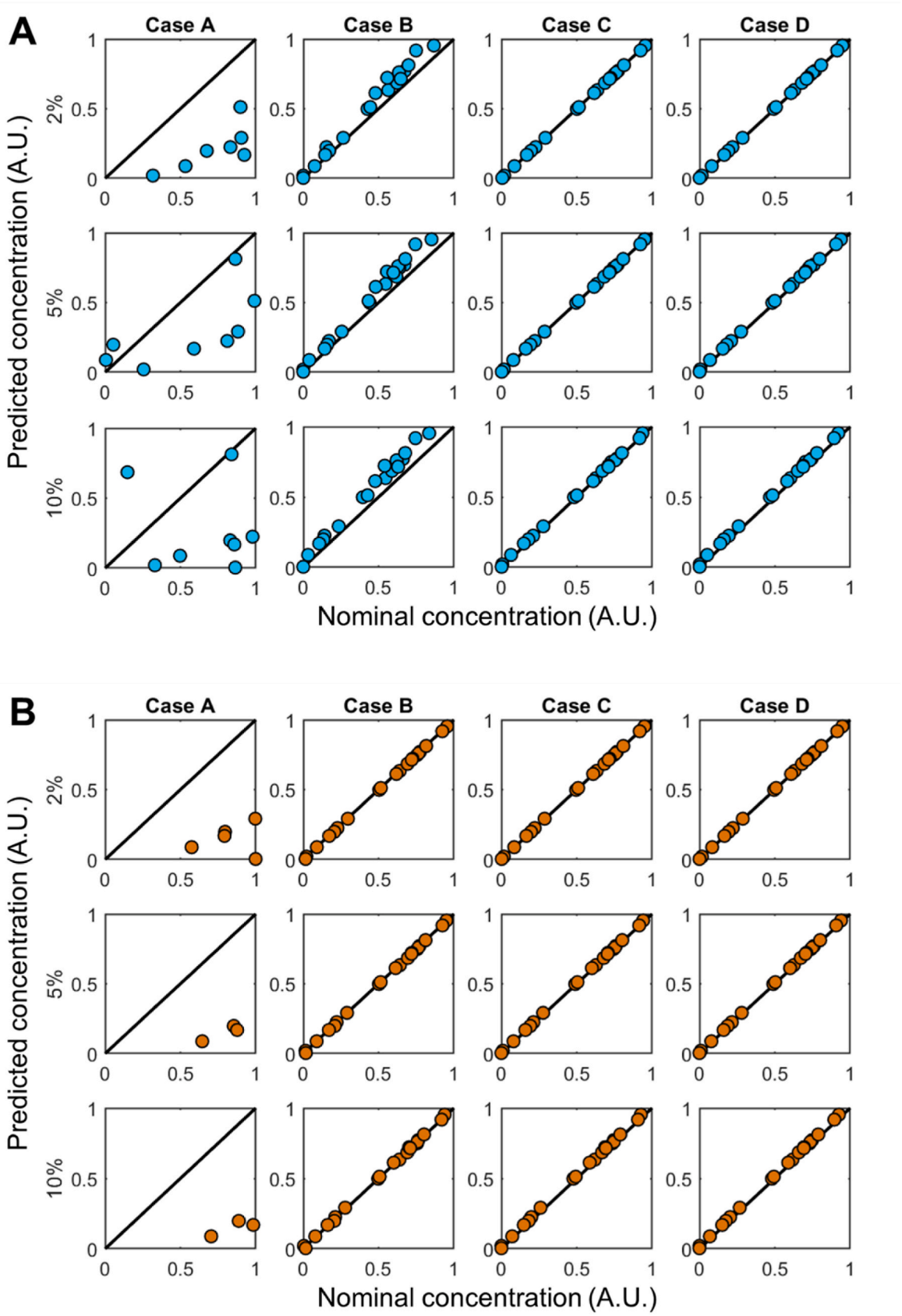

Fig. 2. Predicted vs. nominal analyte 1 concentration in test samples after MCR-ALS modelling of simulated data, according to **A**) S1 and **B**) S2 calibration schemes. (Some samples are not depicted in case A since they fall outside the chosen scale). Each sub-figure corresponds to a given case of local rank (cases A to D) and a level of instrumental noise (2, 5 and 10 % of the mean calibration signal). A.U. means arbitrary units.

The results demonstrate that in cases similar to case A in either S1 or S2, the analytical performance of MCR-ALS is dramatically affected, since the analyte (1 in this case) does not exhibit a window of local rank 1. Notwithstanding, an improvement in the analytical performance is observed while the selectivity pattern is enhanced (from A to D). In this regard, it is interesting to observe that the ability of MCR-ALS to successfully predict the analyte concentration also depends on the calibration strategy. This phenomenon is clearly observed in case B, where significantly biased predictions are obtained when the analyte 2 is present in calibration samples. Hence, in S1, the hypothesis of local rank for analyte 1 is not the only necessary condition that conspires against a successful calibration model. This idea is confirmed in light of the satisfactory predictions in C and D, where both analytes exibit regions of local rank 1. This result establishes a difference from previous observations for systems with only two constituents, and suggests the need to redefine the hypothesis about local rank in three-component systems, when both analytes are to be calibrated together. Moreover, if this condition is fulfilled, the resolution of analyte 1 will be correct regardless of the local rank of the uncalibrated component (interferent), as no significant differences can be observed in the prediction performances of cases C and D. This last issue is consistent with previous results for two-component systems [23,24].

About S2, it is not surprising that when analyte 1 presents a region of local rank 1, satisfactory analytical predictions are always obtained (cases B-D). Indeed, since analyte 2 is only present in the test samples, the three-constituent system can be reduced to a two-component system, in which analyte 2 and the true interferent are modelled as a single component. When this is the selected strategy, the analytical system mimics a calibration problem of one analyte and one interferent, obtaining perfectly equivalent conclusions about MCR-ALS performance, as discussed in previous works.

It is also interesting to notice an issue that becomes evident from a thorough observation of the predicted vs nominal concentrations of analyte 1. It is not obvious that the larger the number of selective sensors the analyte 1 presents, the better the MCR-ALS predictions are obtained: even in successful cases, small biases occur. Preliminary tests, not shown in this work, suggested that the width of the sensor window where the analyte 1 exhibits local rank 1, i.e., the number of selective points, have an effect on the initialisation strategy. The purest variable method is still a matter of study among the chemometric community and further investigation should be conducted to get insights on this phenomenon.

Finally, a fact that deserves attention is that these outcomes are not hindered by the level of instrumental noise. In all cases where the conditions about signal selectivity are met, the REP% values vary proportionally with the percentage of noise.

4.2. Simulated data – RA diagnosis in S1 calibration scheme

The above results can be justified in light of the analysis of the corresponding AFSs. Based on Borgen-Rajkó plots, the following analysis is devoted exclusively to the observations made for simulated systems analogous to S1, for which 3-component MCR-ALS models were obtained. In all simulations, components 1 and 2 refers to the analytes, wheres the component 3 represents the interferent.

Representative Borgen-Rajkó plots, showing AFSs both in the column-space (left) and the row-space (right) for each of the considered cases of local rank are depicted in Fig. 3. In Fig. 3, the spectral (S_1, S_2 and S_3) and concentration (C_1, C_2 and C_3) true profiles utilised in the simulation are depicted using red squares. Furthermore, the initial estimates retrieved by purest variables from the concentration at the purest spectral variables are denoted by magenta circles (Sim_1, Sim_2 and Sim_3). It is important to highlight that the feasible region of each profile is bounded by blue, red, and green regions, while black dots symbolise the data rows and columns. The convergence trajectory of MCR-ALS is illustrated in all panels with blue, red, and green triangles, corresponding to the first, second, and third spectral profiles, respectively. In

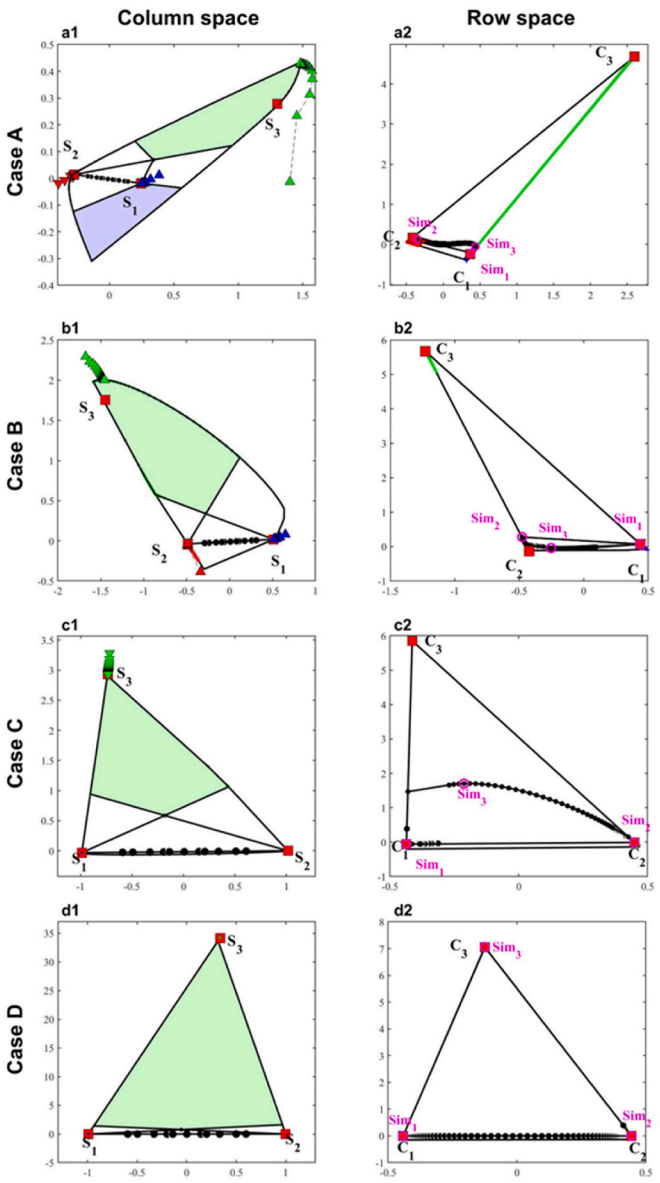

Fig. 3. Borgen-Rajkó plots of generic datasets from S1 calibration scheme, showing the AFS in the column-space (left) and the row-space (right) for each of the considered cases of local rank. Indeces 1 and 2 refers to analaytes, whereas 3 belongs to the interferent. Black circles indicate row/columns coordinates of simulated dataset, while red squares represent true concentrations (C_1, C_2 and C_3) and spectral (S_1, S_2 and S_3) profiles used in the simulation. Coloured areas in blue, red and green highlight feasible solutions for the first, second, and third component. Magenta circles depict the initial estimates retrieved by the purest variables method, with concentration profiles at the purest spectral variables (Sim_1, Sim_2 and Sim_3). Blue, red and green triangles mark alternating least-squares trajectories during convergence. (For interpretation of the references to colour in this figure legend, the reader is referred to the Web version of this article.)

those subfigures where no trajectories with triangles are shown, it is because the algorithm converges in the first iteration. Each pair of panels (1 and 2) illustrate the column and row spaces of cases A to D, respectively, indicating both spectral and concentration domains.

As it can be observed for case A (panels a1 and a2), due to severe overlap in the spectral direction, all the profiles are recovered with ranges that can be explained with Manne theorems [31]. Additionally, due to the lack of local rank 1 in the spectral mode, the initial purest variables (magenta circles in panel a2) diverge from true concentration

profiles (red squares titled C_1, C_2 and C_3). MCR-ALS, starting with concentration profiles at the purest spectral variables, converges to the spectral profile of the interferent, which is different from the true one and finally results in inappropriate calibration outputs. Guided by the duality principle inherent in three-component systems, a reciprocal relationship exists between the analyte concentration and spectral profiles of the second and third components (analyte 2 and interferent). Consequently, any discrepancy in the accuracy of the interferent spectral profile directly impacts the accuracy of the analyte concentration profile and vice versa.

In case B, the pure concentration profile is present in the data columns due to the local rank 1 for the analyte spectral profile. Hence, the initialisation method selects true C_1 as the initial profile (see panel b2). Additionally, the resolution of the spectral profile of the analyte (S_1) is unique due to the Manne theorems, while the others are recovered with ranges [31]. As it is illustrated in panel b1, MCR-ALS converged to true S_1 and S_2 profiles. Finally, the spectral profile of the interferent converges to a point different from the true S_3, resulting in an unacceptable calibration. A comparative analysis of the situation with RA in case B for the S2 calibration scheme can be found in the Supplementary Material.

For case C, there is local rank 1 for both analytes. Hence, initialisation outputs are true concentration profiles of both analytes (see panel c2, where red square and magenta circles are superimposed for the first and the second components). Additionally, based on the uniqueness theorems, the concentration of the interferent (C_3) and spectral profiles of both analytes are unique (see panels c1 and c2). Based on the duality, as the purest variables method selects the true C_1, the spectral space of S_2 and S_3 will be defined uniquely. Besides, this method returns the true C_2 as initialisation; the spectral spaces of S_1 and S_3 are defined unambiguously. Clearly, the definition of these two subspaces resulted in the unique definition of the interferent spectral S_3 subspace. Thuso, MCR-ALS with true C_1 and C_2 converges to true S_3 (see panel c1). Additionally, due to the lack of selectivity of the spectral profile for the interferent, the initialisation output is different from C_3 (see panel c2, where C_3 and Sim_3 are far from each other). Therefore, it takes some ALS steps to converge to true C_3.

Case D has the same unique property as case C with a unique recovery of S_1 and S_2, and C_3. However, in case D, due to the local rank 1 for the spectral profile of the interferent, the true concentration profile of the interferent is among data columns and will be selected by the initialisation method. The only difference is the fast convergence (limited steps) of case D over case C (see MCR-ALS trajectories).

Finally, it is important to mention that extending the study carried out in this work to systems with a greater number of calibrated components is a very complex task due to mathematical and theoretical limitations for the diagnosis of RA. Nevertheless, some hypothesis aimed at generalizing the results for *n*-components systems could be formulated in light of the observations made here. If $n - 1$ analytes are in calibration samples (some of them of pure composition), concentration profiles of each analyte are one of the data columns of the **D** matrix. Additionally, if there are local rank 1 for each analyte spectral profile, then, this condition implies the uniqueness of spectral profiles of all analytes and the concentration profile of the interferent based on the Manne theorem. Hence, if the initialisation is conducted with the concentration profiles at the purest spectral variables, as the concentration profile on $n - 1$ analytes is among data columns, i.e., pure calibration samples and local rank 1, the spectral space of the interferent is recovered uniquely, which has been shown here that is determinant in achieving an accurate calibration.

4.3. Experimental data

Regarding E1, Fig. 4A shows the UV spectra of DCF (analyte 1), CAF (analyte 2) and PAR (interferent). This system exhibits a local rank pattern analogous to that for the simulated case B, in which only analyte 1 presents a window of local rank 1. It can be observed that the width of

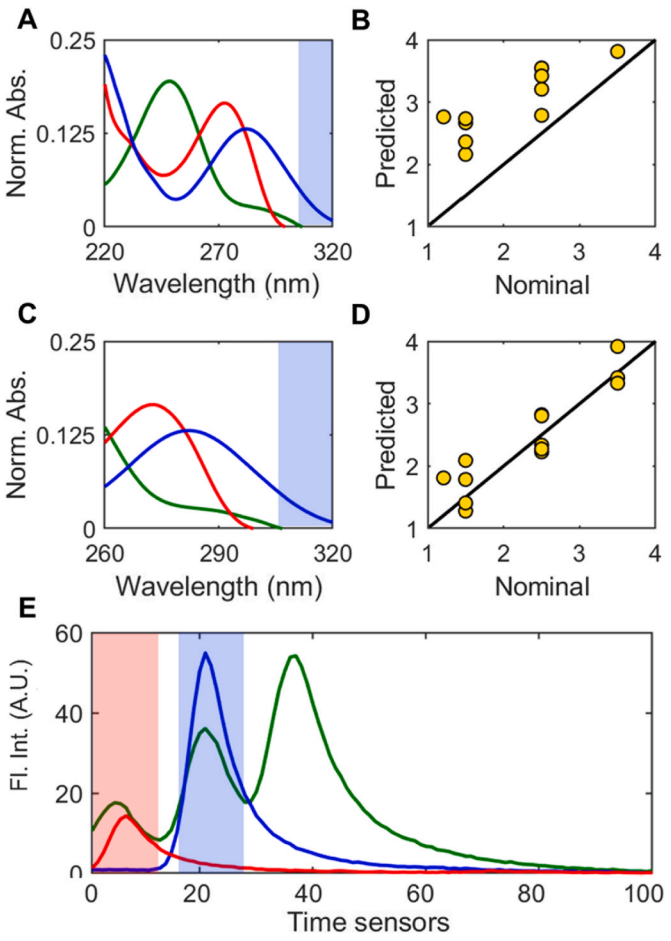

Fig. 4. MCR-ALS outcomes of the experimental datasets. **A.** Normalised pure profiles of DCF (analyte 1, blue), CAF (analyte 2, red) and PAR (interferent, green) considering the whole spectral range of the original dataset, E1 system. **B.** Predicted vs nominal concentrations of DCF in test samples after MCR-ALS decomposition following a calibration scheme of S2 (individual calibration). Concentrations are given in ppm. The black line indicates the identity 1:1 line. **C.** and **D.** are the same as **A** and **B** (respectively), but after selecting the spectral range of 260–320 nm. **E.** Individual chromatograms corresponding to generic samples containing pure CPF (analyte 1, blue), pure OFL (analyte 2, red) and a ternary mixture of both analytes in the presence of DNF (test sample, green), E2 system. (For interpretation of the references to colour in this figure legend, the reader is referred to the Web version of this article.)

the selective point window is significantly smaller (at 300–320 nm/11 sensors) compared to the total spectral length (200–320 nm/101 sensors), which can be deficient in guaranteeing a proper MCR-ALS resolution. The results align with these expectations, since a REP% of 25.5 was obtained (Fig. 4B). In this context, as mentioned before, the width of the window of local rank 1 can be characterised in relative terms as a percentage of selective points. This last parameter can be easily estimated as the ratio between the number of sensors where the contribution to the total signal is only due to the analyte 1 and the total number of signal points of the matrix containing the pure spectra profiles. In simulated datasets, successful cases exhibite percentage of selective points of around 30 % or higher, whereas in E1, the value of this parameter for the DCF is below 20 %. It is worth mentioning that in both types of datasets, the characterisation of the selective region is possible due to the fact that pure profiles and exact composition of test samples are known. This clearly does not constitute a general situation.

For this particular example, it was found that a strategy to improve the performance of MCR-ALS is to increase the % of selective points. It is possible to improve this parameter by selecting a smaller spectral

working region, without losing the information of the other constituents. This fact was confirmed when the restricted spectral region of 260–320 nm (Fig. 4C) was submitted to MCR-ALS. In this case, the new window for analyte 1 rises to 35 % and predictions were significantly improved, obtaining a REP% as low as 9.0 (Fig. 4D). It is very important to remark that this result is only preliminar. As previously mentioned, the effect of the selective region on the prediction capacity is assumed to be related to the selection of purest variables. Additional research is necessary to formulate general conclusions.

At this point, it is relevant to mention that due to the spectral pattern of analyte 2, the simultaneous calibration strategy is not recommended. This observation was confirmed with the results obtained when the S1 type calibration scheme was implemented, for which poor analytical predictions of DCF were obtained (REP% $>$ 20 %). Moreover, if the same methodology is conducted to make predictions of CAF, a very poor analytical performance is obtained (REP% $>$ 70 %), confirming the lack of local rank 1 for this analyte.

The E2 system aims to illustrate the applicability of the proposed methodology to a first-order dataset generated by a different instrumental technique, where the characterisation of the local rank patterns is less intuitive. Fig. 4E shows individual chromatograms corresponding to a sample containing pure CPF (analyte 1), pure OFL (analyte 2) and a ternary mixture of both analytes in the presence of DNF (interferent). As mentioned above, an average R% was calculated to evaluate the prediction capacity of MCR-ALS in this case.

As can be appreciated in Fig. 4E, both analytes exhibit regions of local rank 1. In principle, the system E2 could be modelled considering calibration schemes of either the S1 or S2 types. However, the obtained R% values were 82 and 108 % for S1 and S2, respectively, indicating that predictions are better when analyte 1 is individually calibrated. This result sheds light on the fact that the local rank pattern is less favourable for a calibration strategy of the type of S1 for this particular system, probably due to a lack of local rank of the analyte 2. This example illustrates how analysts could attribute the results to a specific case of local rank on the basis of MCR-ALS predictions, and decide which calibration strategy is the best for a particular analytical problem.

5. Conclusions

There-constituent systems involving first-order data for both a series of simulated and experimental data sets have been exhaustively analyzed with different theoretical and algorithmic techniques. The main findings regarding the ability of MCR-ALS to yield interference-free calibration models in these analytical systems can be summarized as follows: (i) although the rotational ambiguity cannot be completely eliminated, Borgen-Rajkó plots demonstrated that MCR-ALS can retrieve the correct profiles of the analyte of interest under proper initialisation, constraints (non-negativity and correspondence) and specific selectivity patterns, (ii) if both analytes are to be jointly calibrated, both of them must exibit a region of local rank 1, otherwise, the analytes should be individually calibrated if at least one of them exhibits a region of local rank 1, (iii) when the analytes are individually calibrated, the three-component system are reduced to a two-component system and (iv) the proof of concept for first-order datasets can be equivalently extended to unfolded second-order data, which would constitute a general strategy to tackle the problem of non-bilinearity.

Finally, it is important to stress that from the analytical point of view, the possibility of exploiting the second-order advantage with first-order data is highly beneficial, because there is no need to prepare a large and diverse calibration data sets containing all possible interferents. However, in real problems, the success of MCR-ALS will depend on how well the local rank pattern of the analyte of interest is preserved in the different test samples.

Notes

The authors declare no competing financial interest.

CRediT authorship contribution statement

Fabricio A. Chiappini: Writing – review & editing, Writing – original draft, Methodology, Investigation, Formal analysis, Conceptualization. **Licarion Pinto:** Writing – review & editing, Writing – original draft, Software, Methodology, Investigation, Formal analysis, Conceptualization. **Mirta R. Alcaraz:** Writing – review & editing, Writing – original draft, Methodology, Investigation, Formal analysis, Conceptualization. **Nematollah Omidikia:** Raquel Alcaraz: Writing – original draft, Investigation, Formal analysis, Conceptualization. **Hector C. Goicoechea:** Writing – original draft, Methodology, Investigation, Formal analysis, Conceptualization. **Alejandro C. Olivieri:** Writing – original draft, Methodology, Investigation, Formal analysis, Data curation.

Declaration of competing interest

The authors declare that they have no known competing financial interests or personal relationships that could have appeared to influence the work reported in this paper.

Data availability

Data will be made available on request.

Acknowledgments

The authors are grateful to ANPCyT (Agencia Nacional de Promoción Científica y Tecnológica, Projects PICT 2018–02533) and Universidad Nacional del Litoral (CAI + D 2020 N° 50620190100020LI) for financial support. A special thanks to Prof. Aderval Luna from Universidade Estadual do Rio de Janeiro, for contributing to the realization of the collaboration work with Prof. L. Pinto. F.A. Chiappini thanks CONICET for his fellowship.

Appendix A. Supplementary data

Supplementary data to this article can be found online at https://doi.org/10.1016/j.aca.2024.343159.

References

[1] A. de Juan, R. Tauler, Multivariate Curve Resolution: 50 years addressing the mixture analysis problem - a review, Anal. Chim. Acta 1145 (2021) 59–78.
[2] G.M. Escandar, A.C. Olivieri, N.M. Faber, H.C. Goicoechea, A. Muñoz de la Peña, R. J. Poppi, Second- and third-order multivariate calibration: data, algorithms and applications, TrAC, Trends Anal. Chem. 26 (2007) 752–765.
[3] A.C. Olivieri, G.M. Escandar, Chapter 8 - multivariate curve resolution–alternating least-squares, in: A.C. Olivieri, G.M. Escandar (Eds.), Practical Three-Way Calibration, Elsevier, Boston, 2014, pp. 127–156.
[4] W.H. Lawton, E.A. Sylvestre, Self modeling curve resolution, Technometrics 13 (1971) 617–633.
[5] R. Rajkó, Studies on the adaptability of different Borgen norms applied in self-modeling curve resolution (SMCR) method, J. Chemom. 23 (2009) 265–274.
[6] H. Abdollahi, M. Maeder, R. Tauler, Calculation and meaning of feasible band boundaries in multivariate curve resolution of a two-component system, Anal. Chem. 81 (2009) 2115–2122.
[7] R. Rajkó, Additional knowledge for determining and interpreting feasible band boundaries in self-modeling/multivariate curve resolution of two-component systems, Anal. Chim. Acta 661 (2010) 129–132.
[8] R. Rajkó, Some surprising properties of multivariate curve resolution-alternating least squares (MCR-ALS) algorithms, J. Chemom. 23 (2009) 172–178.
[9] A. Golshan, H. Abdollahi, S. Beyramysoltan, M. Maeder, K. Neymeyr, R. Rajkó, M. Sawall, R. Tauler, A review of recent methods for the determination of ranges of feasible solutions resulting from soft modelling analyses of multivariate data, Anal. Chim. Acta 911 (2016) 1–13.
[10] M. Sawall, H. Schröder, D. Meinhardt, K. Neymeyr, 2.12 - on the ambiguity underlying multivariate curve resolution methods, in: S. Brown, R. Tauler,

B. Walczak (Eds.), Comprehensive Chemometrics, second ed., Elsevier, Oxford, 2020, pp. 199–231.
[11] R. Rajkó, H. Abdollahi, S. Beyramysoltan, N. Omidikia, Definition and detection of data-based uniqueness in evaluating bilinear (two-way) chemical measurements, Anal. Chim. Acta 855 (2015) 21–33.
[12] R. Tauler, A. de Juan, Chapter 5 - multivariate curve resolution for quantitative analysis, in: A.M. de la Peña, H.C. Goicoechea, G.M. Escandar, A.C. Olivieri (Eds.), Data Handling in Science and Technology, Elsevier2015, pp. 247-292.
[13] N. Omidikia, M. Ghaffari, J. Jansen, L. Buydens, R. Tauler, Bilinear model factor decomposition: a general mixture analysis tool, Chemometr. Intell. Lab. Syst. 240 (2023) 104901.
[14] G. Ahmadi, H. Abdollahi, A systematic study on the accuracy of chemical quantitative analysis using soft modeling methods, Chemometr. Intell. Lab. Syst. 120 (2013) 59–70.
[15] A.C. Olivieri, N. Omidikia, Initialization effects in two-component second-order multivariate calibration with the extended bilinear model, Anal. Chim. Acta 1125 (2020) 169–176.
[16] R. Rajkó, K. István, Analytical solution for determining feasible regions of self-modeling curve resolution (SMCR) method based on computational geometry, J. Chemom. 19 (2005) 448–463.
[17] M. Sawall, C. Kubis, D. Selent, A. Börner, K. Neymeyr, A fast polygon inflation algorithm to compute the area of feasible solutions for three-component systems. I: concepts and applications, J. Chemom. 27 (2013).
[18] R.B. Pellegrino Vidal, A.C. Olivieri, A new parameter for measuring the prediction uncertainty produced by rotational ambiguity in second-order calibration with multivariate curve resolution, Anal. Chem. 92 (2020) 9118–9123.
[19] A.C. Olivieri, R. Tauler, N-Bands: A new algorithm for estimating the extension of feasible bands in multivariate curve resolution of multicomponent systems in the presence of noise and rotational ambiguity, J. Chemom. n/a e3317.
[20] A.C. Olivieri, Estimating the boundaries of the feasible profiles in the bilinear decomposition of multi-component data matrices, Chemometr. Intell. Lab. Syst. 216 (2021) 104387.
[21] N. Mohseni, M. Bahram, A.C. Olivieri, Second-order advantage obtained from standard addition first-order instrumental data and multivariate curve resolution-alternating least squares. Calculation of the feasible bands of results, Spectrochim. Acta Mol. Biomol. Spectrosc. 122 (2014) 721–730.
[22] C.G. Zampronio, S.P. Gurden, L.A. Moraes, M.N. Eberlin, A.K. Smilde, R.J. Poppi, Direct sampling tandem mass spectrometry (MS/MS) and multiway calibration for isomer quantitation, Analyst 127 (2002) 1054–1060.
[23] F.A. Chiappini, F. Gutierrez, H.C. Goicoechea, A.C. Olivieri, Interference-free calibration with first-order instrumental data and multivariate curve resolution. When and why? Anal. Chim. Acta 1161 (2021) 338465.
[24] F.A. Chiappini, F. Gutierrez, H.C. Goicoechea, A.C. Olivieri, Achieving the analytical second-order advantage with non-bilinear second-order data, Anal. Chim. Acta 1181 (2021) 338911.
[25] F. Allegrini, A.C. Olivieri, Analytical figures of merit for partial least-squares coupled to residual multilinearization, Anal. Chem. 84 (2012) 10823–10830.
[26] B.-V. Grande, R. Manne, Use of convexity for finding pure variables in two-way data from mixtures, Chemometr. Intell. Lab. Syst. 50 (2000) 19–33.
[27] R. Rajkó, Natural duality in minimal constrained self modeling curve resolution, J. Chemom. 20 (2006) 164–169.
[28] L. Pinto, F. Stechi, M.C. Breitkreitz, A simplified and versatile multivariate calibration procedure for multiproduct quantification of pharmaceutical drugs in the presence of interferences using first order data and chemometrics, Microchem. J. 146 (2019) 202–209.
[29] F.v.d. Berg, G. Tomasi, N. Viereck, M.H.G. Amin, F.v.d. Berg, J.-M. Bonny, R. Bro, F. Capozzi, J. Duus, E. Falch, A.G. Ferreira, T. Gostan, B. Hills, N. Howell, P. Hubbard, J. Jaroszewski, L. Kenne, C.-H. Lee, G. Martin, A. Mohoric, N. Nestle, D. Pusiol, S. Rezzi, E.T. Rolls, S.M.D. Shaarani, G.H. Sorland, E. Trezza, E.E. Veliyulin, R.A. Wind, M. Spraul, Warping: investigation of NMR pre-processing and correction, in: P.S. Belton, S.B. Engelsen, H.J. Jakobsen (Eds.), Magnetic Resonance in Food Science, The Royal Society of Chemistry2005, p. 0.
[30] F.A. Chiappini, A. Muñoz de la Peña, H.C. Goicoechea, A.C. Olivieri, An upgrade of MVC2, a MATLAB graphical user interface for second-order multivariate calibration: beyond trilinear models, Chemometr. Intell. Lab. Syst. 237 (2023) 104814.
[31] R. Manne, On the resolution problem in hyphenated chromatography, Chemometr. Intell. Lab. Syst. 27 (1995) 89–94. AUTHOR INFORMATION.